Project 5: Teukolsky Equation on a Kerr Background in Kerr-Schild Coordinates

Graham Reid

November 17, 2014

1 Introduction

The Teukolsky equation describes gravitational, electromagnetic, scalar and neutrino field perturbations of a rotating Kerr black hole. The derivation of both the Teukolsky equation and the Newman-Penrose formalism used is beyond the scope of this project.

2 The Teukolsky Equation

In a 4-dimensional geometry satisfying the Einstein field equations, the curverature of the metric is described by the Weyl tensor, $C_{\alpha\beta\gamma\delta}$, which has 10 independent components [1]. In the Newman-Penrose formalism, these 10 components are given by 5 complex scalars [1]:

$$\Psi_0 = -C_{\alpha\beta\gamma\delta} n^\alpha m^\beta n^\gamma m^\delta \tag{1}$$
$$\Psi_1 = -C_{\alpha\beta\gamma\delta} n^\alpha l^\beta n^\gamma m^\delta \tag{2}$$
$$\Psi_2 = -C_{\alpha\beta\gamma\delta} \bar{m}^\alpha l^\beta n^\gamma m^\delta \tag{3}$$
$$\Psi_3 = -C_{\alpha\beta\gamma\delta} \bar{m}^\alpha l^\beta n^\gamma l^\delta \tag{4}$$
$$\Psi_4 = -C_{\alpha\beta\gamma\delta} \bar{m}^\alpha l^\beta \bar{m}^\gamma l^\delta \tag{5}$$

Here, n, m, l are null vectors chosen to simplify the field equations. In this case, l and n correspond to ingoing in outgoing radial null vectors while m is formed by taking two unit spacelike vectors (perhaps corresponding to vectors in the θ and ϕ directions) and constructing a complex null vector $m^\mu = 1/\sqrt{2}(\mathrm{a}^\mu - ib^\mu)$. In asymptotically flat space with no radiation incoming from infinity, the leading order behaviour of the scalars are [1]:

$$\Psi_0 = O(r^{-5}) \tag{6}$$
$$\Psi_1 = O(r^{-4}) \tag{7}$$
$$\Psi_2 = O(r^{-3}) \tag{8}$$
$$\Psi_3 = O(r^{-2}) \tag{9}$$
$$\Psi_4 = O(r^{-1}) \tag{10}$$

Here we are interested in Ψ_4 as it is the only scalar relevant at infinity and capable of carrying off gravitational wave information. In Boyer-Lindquist coordinates, the background spacetime is given by the Kerr metric [1]:

$$ds^2 = \left(1 - \frac{2Mr}{\Sigma}\right) dt^2 + \left(\frac{4Mar\sin^2\theta}{\Sigma}\right) dtd\phi - \frac{\Sigma}{\Delta} dr^2 - \theta^2 - \sin^2\theta \left(r^2 + a^2 + \frac{2Ma^2 r \sin^2\theta}{\Sigma}\right) d\phi^2 \tag{11}$$

where,

$$\Sigma = r^2 + a^2 cos^2\theta \tag{12}$$
$$\Delta = r^2 - 2Mr + a^2 \tag{13}$$

However, we note that this choice of coordinates is singular at the Schwarzschild radius and is thus a poor choice for studying perturbations of the black hole space time (we want coordinates that allow propagation into the black hole). To achieve this, we define the ingoing-Kerr-Schild coordinates $(\tilde{V}, r, \theta, \tilde{\phi})$ by [1]:

$$r^* = \int \frac{r^2 + a^2}{r^2 - 2Mr + a^2} dr \tag{14}$$
$$\tilde{V} = t + r^* \tag{15}$$
$$\tilde{\phi} = \phi + \int \frac{a}{\Delta} dr \tag{16}$$

Using the tetrad:

$$l^\mu = [\Delta + 4Mr, \Delta, 0, 2a] \tag{17}$$
$$n^\mu = \left[\frac{1}{2\Sigma}, -\frac{1}{2\Sigma}, 0, 0\right] \tag{18}$$
$$m^\mu = \left[ia\sin\theta, 0, 1, \frac{i}{\sin\theta}\right] / (\sqrt{2}(r + ia\cos\theta)) \tag{19}$$

the equation for Ψ_4 may be written [1]:

$$\begin{aligned} 0 = {} & (\Sigma + 2Mr)\,\Psi_{\tilde{t},\tilde{t}} - \Delta\Psi_{r,r} - 6(r - M)\Psi_r - \frac{1}{\sin\theta}(\sin\theta\Psi_\theta)_\theta - \frac{1}{\sin^2\theta}\Psi_{\tilde{\phi},\tilde{\phi}} \\ & -4Mr\Psi_{\tilde{t},r} - 2a\Psi_{r,\tilde{\phi}} + \frac{4i\cot\theta}{\sin\theta}\Psi_{\tilde{\phi}} - (4r + 4ia\cos + 6M)\Psi_{\tilde{t}} + 2(3\cot^2\theta - \csc^2\theta)\Psi \end{aligned} \tag{20}$$

where $\Psi = (r - ia\cos\theta)^4\Psi_4$. To reduce this to a 2+1 form we introduce (replacing all tildes with ordinary characters for the sake of convenience):

$$\Psi(t,r,\theta,\phi) = \sum_m \Phi_m(t,r,\theta)e^{im\phi} \tag{21}$$

The Teukolsky equation for each integer mode m is then given by [1]:

$$\Pi = \Phi_t \tag{22}$$

$$\begin{aligned} 0 = {} & (\Sigma + 2Mr)\,\Pi_t - \Delta\Phi_{r,r} - (2aim + 6r - 6M)\Phi_r - \frac{1}{\sin\theta}(\sin\theta\Phi_\theta)_\theta \\ & -4Mr\Pi_r - (4r + 4ia\cos\theta + 6M)\Pi + (4\cot^2\theta - 2 + m^2\csc^2\theta - 4m\cot\theta\csc\theta)\Psi \end{aligned} \tag{23}$$

3 Azimuthally-Separated Wave Equation in Spherical-Polar Coordinates

Before diving into the Teukolsky equation, we first consider a simple wave equation on Minkowski spacetime to develop the basic principles. We use the usual spherical polar coordinates and adopt the same ansatz for the scalar wave as we did for the Teukolsky equation:

$$\Psi(t,r,\theta,\phi) = \sum_m \Phi_m(t,r,\theta)e^{im\phi} \tag{24}$$

The wave equation, $\nabla^\mu\nabla_\mu\Psi = 0$ may be written:

$$0 = \nabla^\mu\nabla_\mu\Psi \tag{25}$$

$$0 = \frac{1}{\sqrt{-g}}\frac{\partial}{\partial x^\nu}\left(\sqrt{-g}g^{\mu\nu}\frac{\partial\Psi}{\partial x^\mu}\right) \tag{26}$$

$$0 = \sum_m -\frac{\partial^2\Phi_m}{\partial t^2} + \frac{1}{r^2}\frac{\partial}{\partial r}\left(r^2\frac{\partial\Phi_m}{\partial r}\right) + \frac{1}{r^2\sin\theta}\frac{\partial}{\partial\theta}\left(\sin\theta\frac{\partial\Phi_m}{\partial\theta}\right) - \frac{m^2}{r^2\sin^2\theta}\Phi_m \tag{27}$$

which must hold separately for each interger mode m as there is no coupling between levels. We can then define the following system of equations:

$$\frac{\partial\Phi_m}{\partial t} = \Pi_m \tag{28}$$

$$\frac{\partial\Pi_m}{\partial t} = \frac{1}{r^2}\frac{\partial}{\partial r}\left(r^2\frac{\partial\Phi_m}{\partial r}\right) + \frac{1}{r^2\sin\theta}\frac{\partial}{\partial\theta}\left(\sin\theta\frac{\partial\Phi_m}{\partial\theta}\right) - \frac{m^2}{r^2\sin^2\theta}\Phi_m \tag{29}$$

We impose homogeneous Dirichlet conditions at $r = r_{min}$ and approximate Sommerfeld conditions at $r = r_{max}$. At $\theta = 0, \pi$ we require that the relevant functions are smoothly varying ($\frac{\partial\Phi}{\partial\theta} = \frac{\partial\Pi}{\partial\theta} = 0$). Finally we use a time-symmetric

gaussian pulse which is modulated by an appropriate power of $\sin\theta$ to insure that the regularity conditions are satisfied:

$$\Phi(0,r,\theta) = A\exp\left(-\frac{(r-r_0)^2}{\delta r^2}\right)\exp\left(-\frac{(\theta-\theta_0)^2}{\delta\theta^2}\right)\sin^m\theta \quad (30)$$

$$\Pi(0,r,\theta) = 0 \quad (31)$$

Rather than code all of the derivative operators separately it is useful to introduce the following simple operators from which more complex operators can be constructed:

$$D^+f_j = \frac{f_{j+1}-f_j}{\Delta x} \quad (32)$$

$$D^-f_j = \frac{f_j-f_{j-1}}{\Delta x} \quad (33)$$

$$\mu^+f_j = \frac{1}{2}(f_j+f_{j+1}) \quad (34)$$

$$\mu^-f_j = \frac{1}{2}(f_j+f_{j-1}) \quad (35)$$

Centered finite difference operators can then be constructed via application of both derivative operators and averaging operators of the opposite sign. For example:

$$\mu^+D^-f_j = \frac{1}{2}\left(\frac{f_{j+1}-f_j}{\Delta x}+\frac{f_j-f_{j-1}}{\Delta x}\right) = \frac{f_{j+1}-f_{j-1}}{2\Delta x} = \left[\frac{\partial f}{\partial x}\right]_{x=x_j}+O(\Delta x^2) \quad (36)$$

$$D^+D^-f_j = \frac{\frac{f_{j+1}-f_j}{\Delta x}-\frac{f_j-f_{j-1}}{\Delta x}}{\Delta x} = \frac{f_{j+1}-2f_j+f_{j-1}}{\Delta x^2} = \left[\frac{\partial^2 f}{\partial x^2}\right]_{x=x_j}+O(\Delta x^2) \quad (37)$$

$$D^+(\mu^-g_jD^-f_j) = \frac{\frac{1}{2}(g_{j+1}+g_j)\frac{f_{j+1}-f_j}{\Delta x}-\frac{1}{2}(g_j+g_{j-1})\frac{f_j-f_{j-1}}{\Delta x}}{\Delta x} = \frac{(g_{j+1}+g_j)(f_{j+1}-f_j)-(g_j+g_{j-1})(f_j-f_{j-1})}{2\Delta x^2} = \left[\frac{\partial}{\partial x}\left(g(x)\frac{\partial f}{\partial x}\right)\right]_{x=xj} \quad (38)$$

Additionally, we can use these simple operators to define Crank-Nicholson and dissipation operators as follows:

$$\frac{\partial u}{\partial t} = f\left(u,\frac{\partial u}{\partial x}\right)\rightarrow D_t^+u_j^n = \mu_t^+f\left(u_j^n,\mu_x^+D_x^-u_j^n\right) \quad (39)$$

$$\frac{\epsilon\Delta x^4}{16\Delta t}D_x^+D_x^-D_x^+D_x^- = Z_x^\epsilon u_j^n = \frac{\epsilon\Delta x^4}{16\Delta t}D_x^+D_x^-\left[\frac{\partial^2 f}{\partial x^2}\right]_{x=x_j} = \frac{\epsilon\Delta x^4}{16\Delta t}\left[\frac{\partial^4 f}{\partial x^4}\right]_{x=x_j} \quad (40)$$

As in previous projects, we add the dissipation operator to our numeric scheme to damp out high frequency modes which lead to instabilities and are in anycase poorly represented by our numeric scheme.

Now that we have defined our operators, it is possible to write the evolution equations in discrete form [1]:

$$
\begin{aligned}
D_t^+ \Phi^n_{i,j} &= \mu_t^+ \Pi^n_{i,j} + (Z^\epsilon_r + Z^\epsilon_\theta)\Phi^n_{i,j} && (41)\\
D_t^+ \Pi^n_{i,j} &= \mu_t^+ \left[\frac{1}{r_i^2} D_r^+ ((\mu_r^- r_i^2)(D_r^- \Phi^n_{i,j})) \right. \\
&+ \left. \frac{1}{r_i^2 \sin\theta_j} D_\theta^+ ((\mu_\theta^- r_i^2)(D_\theta^- \Phi^n_{i,j})) + \frac{m^2}{r_i^2 \sin^2\theta_j} \Phi^n_{i,j} \right] && (42)\\
&+ (Z^\epsilon_r + Z^\epsilon_\theta)\Pi^n_{i,j} && (43)
\end{aligned}
$$

At the boundaries we will have to modify this expression. For example along the r and θ boundaries we replace the above expression with the relevant boundary conditions while at the points beside the boundary we remove the offending Z^ϵ_α term which requires two available points on either side. Additionally, as a check that we are evaluating the correct expression, we use an independent descritization of the PDE and verify that when applied to our solution, the residual vanishes at the appropriate power of the mesh spacing. In this case, and for the Teukolsky equation, the independent residual evaluator simply expands all derivatives [1]:

$$
\begin{aligned}
D_t^+ \Pi^n_{i,j} &= \mu_t^+ \left[\left(D_r^+ D_r^- + \frac{2}{r_i} D_r^0 + \frac{1}{r_i^2} D_\theta^+ D_\theta^- + \frac{1}{r_i^2 \tan\theta_j} D_\theta^+ \right. \right. && (44)\\
&- \left. \left. \frac{m^2}{r_i^2 \sin^2\theta_j} \right) \Phi^n_{i,j} \right] && (45)
\end{aligned}
$$

3.1 Results

The wave example was downloaded and run and it was verified that the simulation and the independent residual evaluation were convergent.

4 Teukolsky Equation Numerics

Using the spherical wave equation code as a template, a code for the Teukolsky equation was implemented. As RNPL [2] does not support complex numbers, the PDE was rewritten as a system of four, real, first order in time, equations. Due to the length of the equations, I have refrained from explicitly typing them out is this report.

At the boundaries of the region we apply the following conditions in θ,

$$
\begin{aligned}
\left[\frac{\partial F}{\partial \theta} \right]_{\theta=0,\pi} &= 0 \quad \text{m even} && (46)\\
[F]_{\theta=0,\pi} &= 0 \quad \text{m odd} && (47)
\end{aligned}
$$

while at $r = r_{max}$ we apply approximate Sommerfeld conditions,

$$\left[\frac{\partial F}{\partial t} + \frac{\partial F}{\partial r} + \frac{F}{r}\right]_{r=r_{max}} = 0 \tag{48}$$

and use $O(r^3)$ extrapolation to determine the $r = r_{min}$ value.

As the location for the black hole horizon is $r_{BH} = M + \sqrt{M^2 - a^2}$ we require that $a \leq M$ and that $r_{min} \leq r_{BH}$. Additionally, we apply dissipation in both the radial and angular directions as in the wave example and code independent residual evaluators for Π_{Re} and Π_{Im}.

4.1 Convergence and Stability

Using the parameters suggested in [1], it was verified that the simulation and independent residual evaluators converged with the expected power of the mesh spacing (second order Crank-Nicholson). When the code was run for a long period of time however, an instability developed near the black hole horizon. This instability caused the perturbation to grow with time rather than dissipate, eventually causing numeric overflow.

Preliminary investigation revealed that the instability was due to insufficiently fine mesh spacing near the vicinity of the black hole. This was verified by running a simulation with a mush higher mesh density which was free of the instability. Unfortunately, simply increasing the mesh density is a poor fix as the simulation does not require such large densities far from the horizon. By forcing the entire mesh to be so fine, we are wasting valuable computational resources.

Obviously this is an ideal candidate for adaptive mesh refinement, but excluding that possibility, it is possible to introduce an auxiliary variable s such that $r(s)$ is dense near the horizon and sparse far away. Due to its simple derivative I chose to use,

$$r = \exp s + (r_{min} - 1) \tag{49}$$

$$s = \ln\left(r - r_{min} + 1\right) \tag{50}$$

$$\frac{\partial s}{\partial r} = \frac{1}{r - r_{min} + 1} \tag{51}$$

$$\frac{\partial^2 s}{\partial r^2} = \frac{-1}{\left(r - r_{min} + 1\right)^2} \tag{52}$$

$$\tag{53}$$

Upon updating the code to use s rather than r it was observed that the simulation was stable for long times for both $a = 0$ and $a \lessapprox 1$ ($a > 1$ is unphysical). However, due the approximate nature of the outgoing boundary conditions, a portion of the outgoing radiation was reflected backwards leading to rampant growth at large times for small values of s_{max}. By increasing the radial mesh density and allowing s to become large ($r \approx 1000$), this problem was avoided.

4.2 Qualitative results

For $a = 0$ the imaginary and real portions of Φ and Π are decoupled. As our initial conditions are such that the perturbation is real, it remains real as it evolves. For a non zero, the imaginary and real waves are coupled together; Φ and Π become complex as the equations are evolved. Physically, this is associated with the gravitational waves carrying off angular momentum from the black hole.

It is important to note that for meshes with insufficient radial extent, the outgoing radiation boundary conditions are far from exact and result in significant reflection (I believe that there may also be an excessive amount of scattering from the background metric at large r due to the larger mesh spacings and an inability to accurately resolve the outgoing waves). This reflection/backscattering ultimately results in unbounded growth in the vicinity of the horizon, but can be easily curtailed by increasing the value of r_{max} while maintaining the mesh density near the horizon.

4.3 Quasinormal Frequencies

Using a combination of XVS and DV, time profiles of $\Phi_{Re}(r = 10, \theta = \pi/2)$ were extracted. By plotting the long time evolution of these points, it it possible to get an estimate of the quazinormal ring-down frequencies of a Schwarzschild black hole. These profiles, along with fits generated in *gnuplot* are plotted below in Figures 1, 2, 3 and 4. For these particular initial conditions ($\delta r = 2, \delta\theta = 1, r_0 = 10, \theta_0 = \pi/2, A = 1$) we can easily read off the quasinormal frequencies from the plots and note that for $m = 0, 1, 2$ they are very similar in magnitude. Due to time constraints, the dependance of the frequencies on the initial conditions was not investigated.

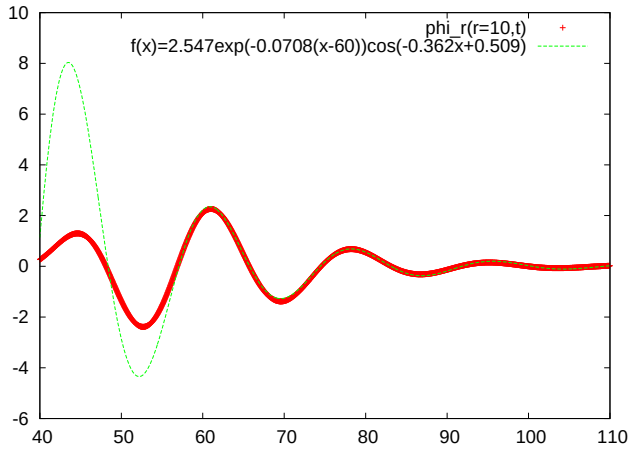

Figure 1: Time profile of $\Phi_{Re}(r = 10, \theta = \pi/2)$ for $m = 0$. The radiation profile eventually settles down into the expected modulated exponential decay. The profile is well fit by an exponential with frequency $\omega = -0.0708i - 0.362$.

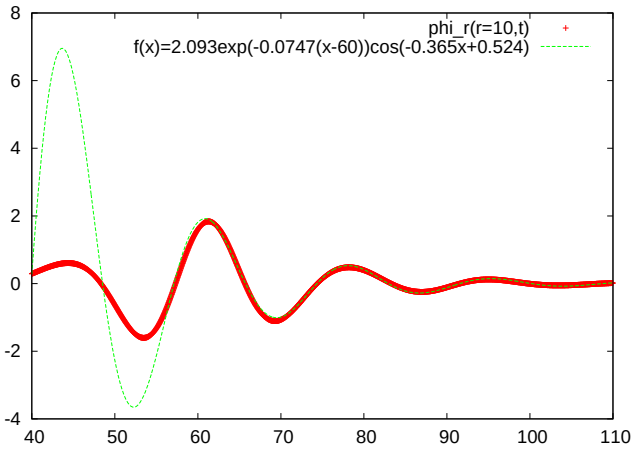

Figure 2: Time profile of $\Phi_{Re}(r = 10, \theta = \pi/2)$ for $m = 0$. The radiation profile eventually settles down into the expected modulated exponential decay. The profile is well fit by an exponential with frequency $\omega = -0.0747i - 0.365$.

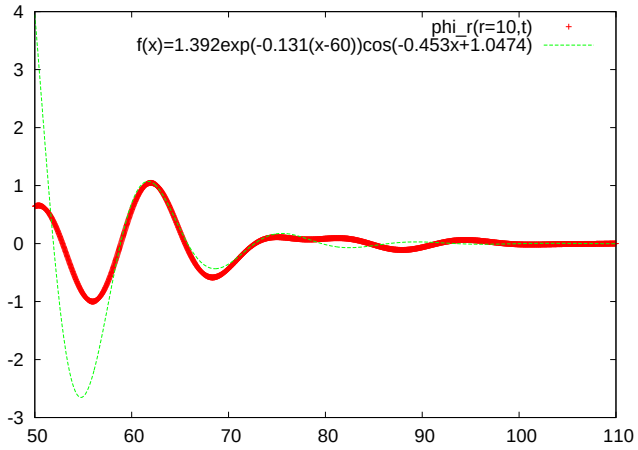

Figure 3: Time profile of $\Phi_{Re}(r = 10, \theta = \pi/2)$ for $m = 0$. The radiation profile doe not settles down into the expected modulated exponential decay, however a closer inspection reveals that there appears to be two modulated exponential decays of similar frequencies contributing to the profile. Figure 4 provides of fit of this data under the assumption that two decays are contributing.

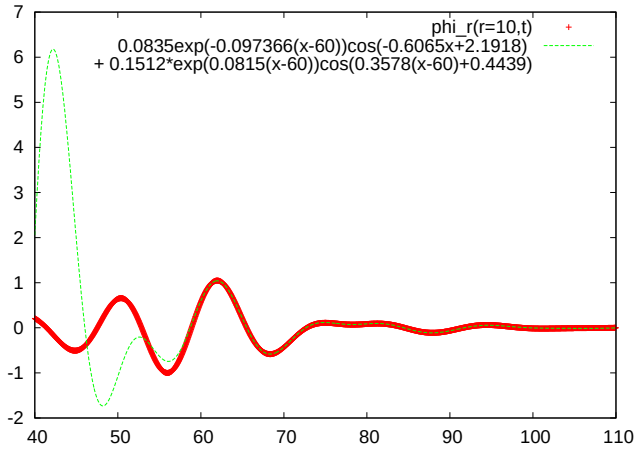

Figure 4: Time profile of $\Phi_{Re}(r = 10, \theta = \pi/2)$ for $m = 0$. The radiation profile settles down into the sum of two modulated exponential decays with similar decay rates. For very long times, the profile will be well fit by an exponential with frequency $\omega = -0.0815i - 0.358$.

References

[1] M. Choptuik, "Project 3(a): Teukolsky equation," http://laplace.physics.ubc.ca/People/matt/Teaching/03Vancouver/p3b.ps, 2011.

[2] M. C. Robert Marsa, "The rnpl reference manual," http://laplace.physics.ubc.ca/People/marsa/rnpl/refman/refman.html, 1995.